GRL MS#3352-r

Plasma waves in the dayside polar cap boundary layer: Bipolar and monopolar electric pulses and whistler mode waves

B. T. Tsurutani, [1] J. K. Arballo, [1] G. S. Lakhina, [1,3] C. M. Ho, [1] B. Buti, [1] J. S. Pickett, [2] D. A. Gurnett, [2]

Abstract. We report four different types of plasma waves detected in and near the dayside polar cap boundary layer (PCBL) region at high altitudes ($> 6\ R_E$). One wave type is narrowband whistler-mode emission at frequencies just below f_{ce} (5.5 kHz). These emissions could be locally generated by resonant wave-particle interactions involving an electron beam of ~100 eV energy. A second type is a low frequency (200-300 Hz) whistler mode wave, which may be locally generated by ~25 keV electrons or ~45 keV ions. It is also possible that these latter waves are generated at low altitudes near the ionosphere and then converted from the ion cyclotron mode into whistler-mode during propagation from the generation region to the spacecraft. Two further types of waves are large-amplitude bipolar and monopolar solitary "electrostatic" waves. The bipolar wave structures are possibly generated all along the magnetic field lines in the field-aligned current regions (at all local times). The monopolar structures could be evolved bipolar solitary waves. A one-d schematic is presented to explain the paired monopolar structures as a result of splitting of an electron hole into two parts.

Introduction

Plasma waves in the low-latitude magnetopause boundary layer (LLBL) [*Gurnett et al.*, 1979; *Tsurutani et al.*, 1981, 1989; *Rezeau et al.*, 1989] and of the polar cap boundary layer (PCBL) [*Tsurutani et al.*, 1998], appear from time-averaged spectra to be broad-banded in both E' and B' (the PCBL has been defined as the region adjacent to the polar cap open magnetic field lines). It is thought that the LLBL and PCBL regions are on the same magnetic field lines. The magnetic component of the broadband waves (B') extends from 10 Hz up to the electron-cyclotron frequency (f_{ce}). The electric component (E') extends from 10 Hz to well above f_{ce}. From the frequency ranges and results of B'/E' analyses, it has been concluded that the boundary layer waves must be a mixture of electromagnetic whistler mode waves plus electrostatic waves [*Tsurutani et al.*, 1998]. However, the exact nature of these waves has remained a mystery.

The purpose of this paper is to examine the PCBL waves in much greater detail using high-time resolution POLAR data [*Gurnett et al.,* 1995]. This paper is a report on our initial findings.

Data Modes

Plasma wave data from two intervals are analyzed. The instrument was in a high telemetry rate mode, so that details of the wave modes could be identified and analyzed. For one interval, the instrument was recording the outputs from the three orthogonal electric (E') antenna signals and also the three orthogonal search coil (B') signals through the High Frequency Waveform Receiver (HFWR). The search coils have a resonant frequency of ~7 kHz, so the sensors are not sensitive to signals well above this frequency. For the other interval, the instrument monitored the magnetic loop output (B') from the Wideband Receiver (WBR). During this interval, only the single axis loop data were available. The loop is much more sensitive to high frequency magnetic signals.

Results

Figure 1 shows the wave parallel and perpendicular components for E' and B' relative to the background magnetic field from 08:27:17.12 to 08:27:17.20 UT (0.08 s), on May 20, 1996. The spacecraft was at 6.1 R_E, 80° invariant latitude and 11:48 magnetic local time when the spacecraft crossed the PCBL region from the magnetosphere into the polar cap region. Several wave features can be noted from Figure 1. The left side of the interval is dominated by high frequency magnetic signatures while the right side has large amplitude electric signals. This "rapid switching of wave modes" is quite common in the data set.

The high frequency magnetic waves (left side) come in bursts or packets. One packet is expanded at the bottom of the figure. It consists of narrowband electromagnetic waves of frequency ~4.9 kHz (power spectra not shown). Wave polarization analysis show that the waves are right-hand polarized and the local f_{ce} is 5.5 kHz. Since these waves are propagating at frequencies slightly below f_{ce}, they are most likely whistler-mode waves. These waves may be auroral hiss [*Gurnett,* 1991], but detected at high altitude.

A second wave mode detected by the single B' loop antenna is shown in Figure 2. It is also electromagnetic in nature. The dominant frequency is ~200-400

Hz. The local f_{ce} is 8.1 kHz and the local proton cyclotron frequency (f_{cp}) is 4.4 Hz. The lower hybrid frequency ($\sim(f_{ce} \cdot f_{cp})^{1/2}$) $\approx$ 190 Hz. We call these signals LFEWS-Low Frequency Electromagnetic Wave Signals. The signals were detected at 5.6 R_E, 80° invariant latitude and 11:56 magnetic local time. Since the wave frequency is between the local f_{cp} and the local f_{ce} and above f_{lh}, these waves also appear to be propagating in the whistler mode.

From the power spectral analysis of this interval, we find that ~2-6 kHz waves are superposed on the LFEWS. This is also shown at the bottom of Figure 2.

A third type of signal detected from the electric antennas and the search coils is shown in Figure 3. These are large amplitude electric "bipolar" pulses (bpp) with typical durations of ~1 ms or less. Clear bipolar pulses can be noted at ~17.331 s, ~17.344 s and ~17.345 s after 08:27:00 UT on May 20, 1996. Bipolar structures are mainly present in the $E'_{\|}$ components. The pulse polarities on the $E'_{\|}$ component are the same, negative first and then positive.

There are (search coil) magnetic signatures associated with the electric pulses. These can be most easily noted when the electric field is large and it changes slowly. An example is noted at 17.352 s and 17.355 s in $B'_{\perp}$. This indicates that there are at times, possibly magnetic variations with the "electrostatic" pulses.

"Offset" bipolar pulses (obpp) are also detected. The positive pulse does not follow immediately after the negative pulse, but is delayed somewhat. Examples can be found at ~17.319 s and 17.320 s.

The bipolar electric signatures are not always isolated. There are times when several occur in a sequence. During these times, the polarities are generally the same.

"Monopolar" electrostatic pulses are shown in the right-hand inset of Figure 3. Positive pulses can be noted at 17.377 s, 17.383 s and 17.387 s (a double pulse) after 08:27:00 UT. Negative pulses occur between the positive pulses: at 17.380 s and 17.385 s. To date, the monopolar pulses are always found to alternate between one polarity and the opposite polarity, and to occur in pairs. Note that in this Figure there is little correspondence between $E'_{\|}$ and $B'_{\perp}$.

Summary of Observations

We have illustrated the presence of several clear types of wave modes/phenomena that are present in the dayside PCBL region at distances of ~6-7 R_E from Earth. The identification of these modes can explain the broadband nature of the time-averaged E' and B' spectra published earlier. It is clear that there are at least several different bands (in frequency) of electromagnetic whistler mode waves. A band at ~200-400 Hz and another at ~5 kHz were illustrated. If the "switching" of bands occurs rapidly in time and the frequencies are variable, a broad whistler spectrum will result. There are also very short time scale "electrostatic" bipolar and monopolar signals. The fast variations in the electric field clearly represent "power" in the high frequency domain, giving a broad range of electrostatic "wave" power. *Matsumoto et al.* [1994] have clearly shown this to be the case for plasmasheet boundary layer Broadband Electrostatic Noise (BEN) signals.

Instabilities

The high frequency electromagnetic waves are clearly propagating in the whistler mode. The waves could be generated by a local resonant wave-particle interaction process involving electron or ion beams. We can estimate the resonant energy by assuming the first-order cyclotron resonant condition:

$$\omega - k_{\|} V_{\|} = n\Omega$$

where ω corresponds to the wave frequency (in rad s^{-1}), Ω, the cyclotron frequency (in rad s^{-1}), $k_{\|}$ and $V_{\|}$ the parallel components of the wave vector and particle velocity, respectively, and n is an integral multiple ($n = 0, \pm 1, \ldots$) of the particle gyrofrequency. Based on the B'/E' estimates, the wave phase speed (ω/k) is approximately taken as $10^{-2}c$ (*Tsurutani et al.* [1998], Figure 7), where c is the speed of light (we note that the wave phase-speed varies as a function of angle of propagation relative to, and as a function of, frequency, so there are uncertainties in the above value). For normal cyclotron resonance (right-hand rotating electrons in resonance with right-hand whistler mode waves), there are two possibilities: a) the waves and particles are propagating in the same direction with the waves overtaking the particles, and b) the waves and particles are propagating in opposite directions. For the former case, the resonant energy is ~100 eV. For the latter case, the resonant energy is too low to be physically meaningful. Another possibility is that the waves are generated remotely, say in the ionosphere. Generation by ions by an anomalous cyclotron resonance (left-hand rotating ions overtaking right-hand waves) is also possible. For the latter to occur, the resonant energies would be ~50 keV. Discussion of resonant and anomalously resonant interactions can be found in *Thorne and Tsurutani* [1987] and *Tsurutani and Lakhina* [1997]. The next step is to search for simultaneous particle data to determine if there are ~100 eV electron beams or ~50 keV ion beams present or not. This effort will be undertaken soon.

The source of the LFEWS (200-400 Hz) is more difficult to determine. The waves appear to be whistler mode, but there are a variety of particles that could be responsible for generating the waves. Counter-streaming resonant electrons would have energies of ~25 keV. Parallel propagating ion beams for anomalously resonant interactions (the ions are propagating parallel to and overtaking the waves) would have parallel energies of ~45 keV. A third possibility is initial left-hand wave generation (through ions), with later wave mode conversion (from left to right). Such a scenario would have wave generation in a left-hand mode near the ionosphere by a source such as ion conics. The waves would propagate towards the ionosphere to a region where crossover is possible, and then reflect back into the outer magnetosphere. The interesting part of this scenario is that the f_{cp} in the polar ionosphere is ~800 Hz, quite consistent with the observations of ~200-400 Hz waves. *Mozer et al.* [1997] have detected such ion cyclotron waves at Polar perigee altitudes (~5000 km) in the dawn auroral zone. The waves were associated with an upgoing ~1 keV ion beam.

Although the detection of bipolar "electrostatic" structures in the nightside auroral zone at low altitude is well documented [*Temerin et al.,* 1982; *Ergun et al.,* 1998], the discovery of bipole "electrostatic" structures in the dayside PCBL at large distances from the auroral ionosphere is somewhat of a surprise (see also *Franz et al.* [1998]). One obvious possible explanation is that bipolar structures are generated in field-aligned current regions at all local times and all altitudes along the magnetic field line. Although a statistical study has not been completed, *Franz et al.* [1998] have detected bipolar "electrostatic" structures from 2 to 8.5 R_E.

These three types of parallel electric field (bipolar, offset bipolar and monopolar, from left to right) structures are sketched in Figure 4. Assuming an electron hole [*Franz et al.,* 1998] and neutralizing charge are responsible for the bipolar electric structures, we show a 1-d sketch of the spatial distribution of charge. The spacecraft is assumed to fly through the center of this distribution, resulting in the electric field signature detected by Polar. The middle panels show an "offset" bipolar structure and a possible charge distribution that could result in the observed electric fields. This plasma structure would be essentially a "broadened" electron hole, perhaps due to dispersion effects. At the right of Figure 4, we show a pair of monopolar pulses. The corresponding possible charge distribution is that of a split electron hole. Hole splitting has been theoretically shown to occur via interaction with density gradients [*Mohan and Buti,* 1979].

What is interesting in these three types of structures is that they may be related. The offset bipolar structures and the paired monopolar structures may be evolutionary states of the bipolar pulses. Clearly more work is needed to understand if this possibility is correct or not.

Conclusions

We have shown that the dayside PCBL region is an exciting one for instabilities and nonlinear waves. The monopolar "electrostatic" structures should give very interesting clues to experimentalists and challenges to theorists. Wave-particle interactions with solitary "bipolar" and "monopolar" features need to be examined carefully. Particle and wave correlations have been noted [*Tsurutani et al.,* 1998], and particle acceleration by interaction with these waves is likely. Finally, we should mention that new missions exploring far regions of space such as the Solar Probe mission going to 4 R_S from the Sun should consider having instrumentation capable of detecting such waves. Since the prime objective of the Solar Probe mission is to determine the heating of the solar corona and acceleration of the solar wind, such wave-particle interactions might be highly relevant.

Acknowledgments. Portions of this research were done at the Jet Propulsion Laboratory, California Institute of Technology, under contract with NASA. BTT wishes to thank R.E. Ergrun for helpful scientific discussions. Both GSL and BB would like to thank the NRC for the awarding of SRR Associateships at JPL. JSP and DAG acknowledge support from NASA/GSFC under contract NAS5-30371.

References

Ergun, R.E., C.W. Carlson, J.P. McFadden, et al., FAST satellite observations of large-amplitude solitary structures, *Geophys. Res. Lett., 25,* 2041, 1998.

Franz, J.R., P.M. Kintner and J.S. Pickett, POLAR observations of coherent electric field structures, *Geophys. Res. Lett., 25,* 1277, 1998.

Gurnett, D.A., Auroral plasma waves, in *Auroral Physics,* edited by C.I.-Meng, M.J. Rycroft and L.A. Frank, Cambridge Univ. Press, 1991.

Gurnett, D.A., R.R. Anderson, B.T. Tsurutani, et al., Plasma wave instabilities at the magnetopause: Observations from ISEE 1 and 2, *J. Geophys. Res., 84,* 7043, 1979.

Gurnett, D.A., A.M. Persoon, R.F. Randall, et al., The Polar plasma wave instrument, *Space Sci. Rev., 71,* 597, 1995.

Matsumoto, H., H. Kojima, T. Miyatake, et al., Electrostatic solitary waves (ESW) in the magnetotail - BEN wave forms observed by GEOTAIL, *Geophys. Res. Lett., 21*, 2915, 1994.

Mohan, M. and B. Buti, Modulated ion acoustic waves in inhomogeneous plasmas, *Plasma Phys., 21*, 713, 1979.

Mozer, F.S., R. Ergun, M. Temerin, New features of time domain electric-field structures in the auroral acceleration regions, *Phys. Rev. Lett., 79*, 1281, 1997.

Rezeau, L., A. Morane, S. Perraut, et al., Characterization of Alfvénic fluctuations in the magnetopause boundary layer, *J. Geophys. Res., 94*, 101, 1989.

Temerin, M., K. Cerny, W. Lotko, et al., Observations of double layers and solitary waves in the auroral plasma, *Phys. Rev. Lett., 48*, 1175, 1982.

Thorne, R.M. and B.T. Tsurutani, Resonant interactions between cometary ions and low frequency electromagnetic waves, *Planet. Space Sci., 35*, 1501, 1987.

Tsurutani, B.T., E.J. Smith, R.M. Thorne, et al., Wave-particle interactions at the magnetopause: Contributions to the dayside aurora, *Geophys. Res. Lett., 8*, 183, 1981.

Tsurutani, B.T., A.L. Brinca, E.J. Smith, et al., A survey of ELF-VLF plasma waves at the magnetopause, *J. Geophys. Res., 94*, 1270, 1989.

Tsurutani, B.T., and G.S. Lakhina, Some basic concepts of wave-particle interactions in collisionless plasmas, *Rev. Geophys., 35*, 491, 1997.

Tsurutani, B.T., G.S. Lakhina, C.M. Ho, et al., Broadband plasma waves observed in the polar cap boundary layer: POLAR, *J. Geophys. Res., 103*, 17351, 1998.

J. K. Arballo, B. Buti, C. M. Ho, G. S. Lakhina, and B. T. Tsurutani, Jet Propulsion Laboratory, California Institute of Technology, Pasadena, CA 91109. (e-mail: Bruce.Tsurutani@jpl.nasa.gov)

D. A. Gurnett and J. S. Pickett, Department of Physics and Astronomy, 203 Van Allen Hall, University of Iowa, Iowa City, Iowa 52242-1479.

(Received June 22, 1998; revised September 16, 1998; accepted September 18, 1998.)

---

[1]Jet Propulsion Laboratory, Pasadena, California.

[2]Department of Physics and Astronomy, University of Iowa, Iowa City, Iowa.

[3]Permanently at Indian Institute of Geomagnetism, Colaba, Bombay-400005, India.

Figure 1. Whistler-mode wave E' and B' parallel and perpendicular components relative to the background magnetic field. The inset shows a wave packet with frequency at ~4.9 kHz.

Figure 1. Whistler-mode wave E' and B' parallel and perpendicular components relative to the background magnetic field. The inset shows a wave packet with frequency at ~4.9 kHz.

Figure 2. Low frequency magnetic waves detected from a single B' loop antenna from 11:35:25.75 to 11:35:26.00 UT on May 14, 1996. The dominant frequency is ~200-400 Hz.

Figure 2. Low frequency magnetic waves detected from a single B' loop antenna from 11:35:25.75 to 11:35:26.00 UT on May 14, 1996. The dominant frequency is ~200-400 Hz.

Figure 3. Bipolar (bpp), offset bipolar (obpp), and monopolar (mpp) wave structures in $E'_{\parallel}$.

Figure 3. Bipolar (bpp), offset bipolar (obpp), and monopolar (mpp) wave structures in $E'_{\parallel}$.

Figure 4. A schematic showing a bipolar electric field structure (left), an offset bipolar structure (middle), and a pair of oppositely polarized monopolar structures (right). The bipolar pulse is modeled by an electron hole plus surrounding neutralizing charge. The offset bipolar pulse is modeled by a broadened electron hole. The two monopolar pulses are modeled by an electron hole that has split into two parts.

Figure 4. A schematic showing a bipolar electric field structure (left), an offset bipolar structure (middle), and a pair of oppositely polarized monopolar structures (right). The bipolar pulse is modeled by an electron hole plus surrounding neutralizing charge. The offset bipolar pulse is modeled by a broadened electron hole. The two monopolar pulses are modeled by an electron hole that has split into two parts.

TSURUTANI ET AL.: PLASMA WAVES IN THE DAYSIDE PCBL

TSURUTANI ET AL.: PLASMA WAVES IN THE DAYSIDE PCBL

TSURUTANI ET AL.: PLASMA WAVES IN THE DAYSIDE PCBL

TSURUTANI ET AL.: PLASMA WAVES IN THE DAYSIDE PCBL

TSURUTANI ET AL.: PLASMA WAVES IN THE DAYSIDE PCBL

TSURUTANI ET AL.: PLASMA WAVES IN THE DAYSIDE PCBL

TSURUTANI ET AL.: PLASMA WAVES IN THE DAYSIDE PCBL

TSURUTANI ET AL.: PLASMA WAVES IN THE DAYSIDE PCBL

TSURUTANI ET AL.: PLASMA WAVES IN THE DAYSIDE PCBL

TSURUTANI ET AL.: PLASMA WAVES IN THE DAYSIDE PCBL

TSURUTANI ET AL.: PLASMA WAVES IN THE DAYSIDE PCBL

TSURUTANI ET AL.: PLASMA WAVES IN THE DAYSIDE PCBL

TSURUTANI ET AL.: PLASMA WAVES IN THE DAYSIDE PCBL

TSURUTANI ET AL.: PLASMA WAVES IN THE DAYSIDE PCBL

TSURUTANI ET AL.: PLASMA WAVES IN THE DAYSIDE PCBL

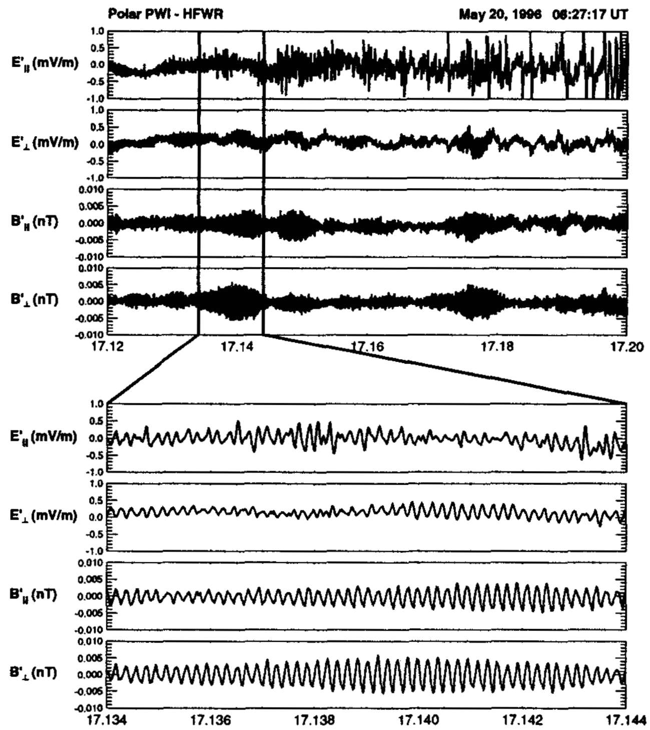

Polar PWI - HFWR
May 20, 1996 06:27:17 UT
E'∥ (mV/m)
E'⊥ (mV/m)
B'∥ (nT)
B'⊥ (nT)
17.12
17.14
17.16
17.18
17.20
17.134
17.136
17.138
17.140
17.142
17.144

Figure 1

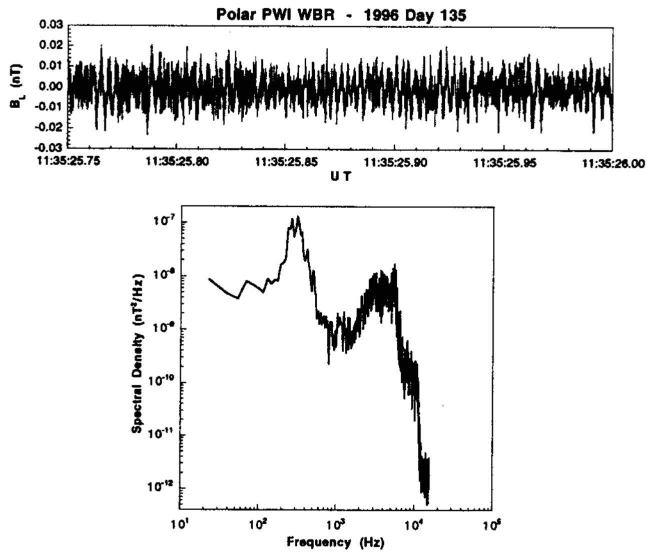

Polar PWI WBR - 1996 Day 135
0.03
0.02
0.01
0.00
-0.01
-0.02
-0.03
B_L (nT)
11:35:25.75
11:35:25.80
11:35:25.85
11:35:25.90
11:35:25.95
11:35:26.00
U T
10^{-7}
10^{-8}
10^{-9}
10^{-10}
10^{-11}
10^{-12}
Spectral Density (nT^2/Hz)
10^{1}
10^{2}
10^{3}
10^{4}
10^{5}
Frequency (Hz)

Figure 2

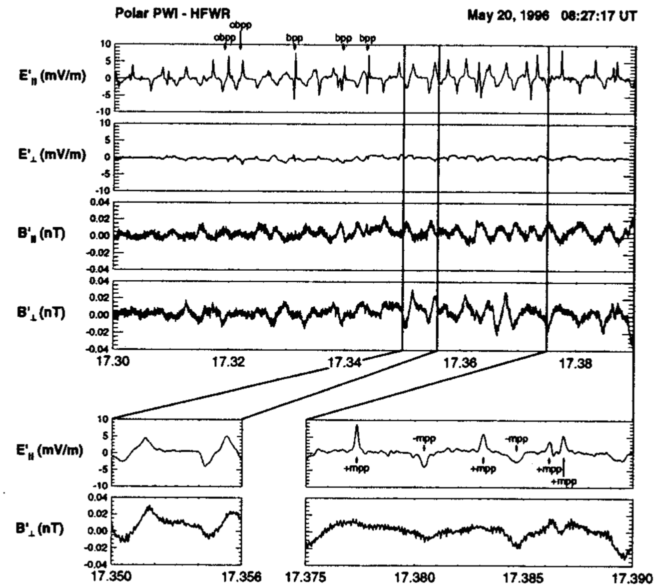

Polar PWI - HFWR
May 20, 1996 08:27:17 UT
E'∥ (mV/m)
E'⊥ (mV/m)
B'∥ (nT)
B'⊥ (nT)
obpp
bpp
-mpp
+mpp
17.30
17.32
17.34
17.36
17.38
17.350
17.356
17.375
17.380
17.385
17.390

Figure 3

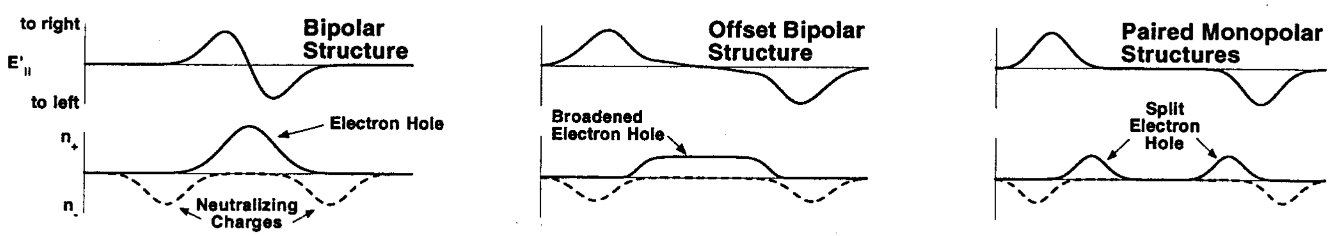
to right
E'∥
to left
Bipolar Structure
Electron Hole
n_+
n_-
Neutralizing Charges
Offset Bipolar Structure
Broadened Electron Hole
Paired Monopolar Structures
Split Electron Hole

Figure 4